

The Effect of the Frontal Plane Tibiofemoral Angle and Varus Knee Moment on the Contact Stress and Strain at the Knee Cartilage

Nicholas H. Yang, Paul K. Canavan, and Hamid Nayeb-Hashemi

Subject-specific models were developed and finite element analysis was performed to observe the effect of the frontal plane tibiofemoral angle on the normal stress, Tresca shear stress and normal strain at the surface of the knee cartilage. Finite element models were created for three subjects with different tibiofemoral angle and physiological loading conditions were defined from motion analysis and muscle force mathematical models to simulate static single-leg stance. The results showed that the greatest magnitude of the normal stress, Tresca shear stress and normal strain at the medial compartment was for the varus aligned individual. Considering the lateral knee compartment, the individual with valgus alignment had the largest stress and strain at the cartilage. The present investigation is the first known attempt to analyze the effects of tibiofemoral alignment during single-leg support on the contact variables of the cartilage at the knee joint. The method could be potentially used to help identify individuals most susceptible to osteoarthritis and to prescribe preventive measures.

Keywords: varus, tibiofemoral, knee, finite element

Osteoarthritis (OA) is a degenerative disease of articular cartilage that affects approximately 21 million people and costs the U.S. economy over \$60 billion per year (www.orthoinfo.aaos.org). Several reported symptoms of OA include limited mobility, pain and joint deformity (Arokoski et al., 2000). It is a common belief that both systemic and biomechanical factors contribute to OA development in a joint. Factors, such as age, sex, racial characteristics, and genetics define the mechanical properties of the cartilage (Felson & Zhang, 1998; Felson, 1999; Sowers, 2001; Arokoski et al., 2000). However, experimental studies have shown that excessive loading on the cartilage can cause damage that could lead to OA initiation and progression (Repo & Finlay, 1977; Kerin et al., 1998; Quinn et al., 2001; Clements et al., 2001; Chen et al., 2003; Morel et al., 2006). Local biomechanical factors (joint loading, joint injury, joint deformity, meniscectomy, alignment, etc.) may also severely affect the initiation and progression of OA due to abnormal loading conditions at the joint (Felson & Zhang, 1998; Felson, 1999; Cooper et al., 2000; Sharma et al., 2000; Sharma,

2001; Sowers, 2001; Arokoski et al., 2000; Cerejo et al., 2002; Englund & Lohmander, 2004; Felson, 2005; Griffin & Guilak, 2005).

Obesity combined with tibiofemoral alignment has been associated with increased progression of knee OA (Felson & Zhang, 1998; Felson, 1999; Sharma et al., 2000, 2001; Sharma, 2001; Cerejo et al., 2002; Englund & Lohmander, 2004; Felson, 2005; Griffin & Guilak, 2005). Tibiofemoral alignment affects the varus/valgus moment during ambulation and during single-leg stance. The tibiofemoral alignment at the knee is measured by the angle formed by the intersection of the anatomical axes of the femur and the tibia, Figure 1. A "normal" knee will have a tibiofemoral angle of approximately 5–7° valgus (Johnson et al., 1980; Karachalios et al., 1994). Deviation from this angle leads to a knee joint with varus or valgus condition. A varus aligned knee is described as "bow-legged" with an angle less than 5° valgus. A valgus aligned knee is described as "knocked-kneed" with an angle greater than 7° valgus.

In normal knee alignment, approximately 70–75% of the load passes to the medial compartment during walking (Hsu et al., 1988; Andriacchi, 1994; Andriacchi et al., 2004). The varus moment, or adduction moment, is the primary factor in the distribution of the force to the medial compartment of the knee joint during normal gait (Andriacchi, 1994; Andriacchi et al., 2004; Shelburne et al., 2005; Schipplein & Andriacchi, 1991; Zhao et al., 2006, 2007). The varus knee moment is dependent on the location of the ground reaction force vector and the location of the center of the knee. A varus aligned knee

Nicholas H. Yang (*Corresponding Author*) is with the Mechanical and Industrial Engineering Dept., Northeastern University, Boston, MA; Yang is now with Exponent, Inc. Paul K. Canavan is with the Physical Therapy Dept., Northeastern University, Boston, MA, and the Department of Physical Therapy, Windham Community Memorial Hospital, Windham, Connecticut. Hamid Nayeb-Hashemi is with the Mechanical and Industrial Engineering Dept., Northeastern University, Boston, MA.

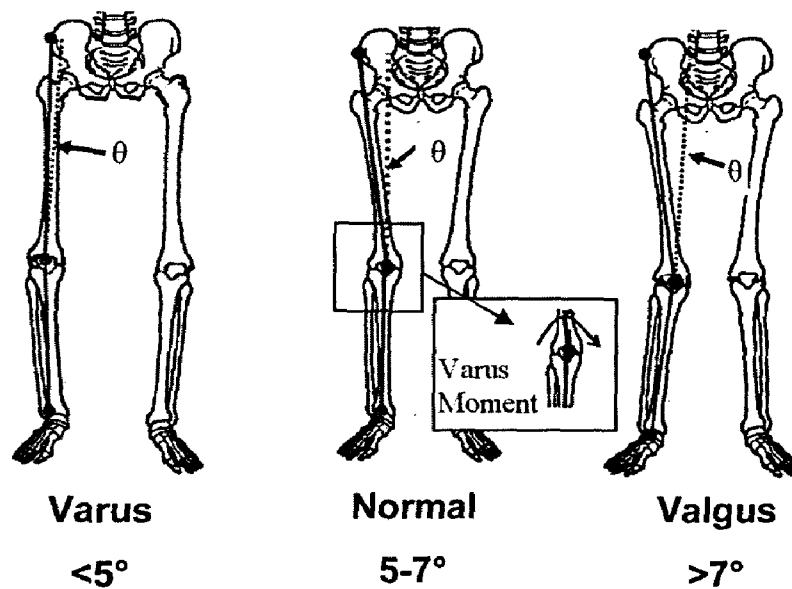


Figure 1 — Frontal plane tibiofemoral angle measured at the intersection of the axis of the femur and the tibia. The inset shows that varus moment at the knee that occurs during the single-leg support. Varus or “bow-legged” alignment has an angle less than 5° , normal alignment is $5\text{--}7^\circ$ and valgus or “knocked-knee” is greater than 7° .

will have a moment that increases the loading on the medial compartment of the knee and a valgus knee will have a moment that increases the loading on the lateral compartment of the knee. However, only in extremely malaligned valgus knees (approximately 15° valgus) will the lateral knee compartment experience more load than the medial knee compartment (Johnson et al., 1980; Sharma et al., 2000).

Individuals who demonstrate a varus knee alignment have been shown to increase the risk of medial compartment OA progression and valgus alignment has been shown to increase the risk of lateral OA progression in as little as 18 months (Sharma et al., 2001). It is not entirely clear if varus/valgus alignment is a cause or a result of knee OA but animal data supports a link between preexisting varus/valgus alignment and OA initiation (Tetsworth & Paley, 1994; Sharma et al., 2001). Furthermore, the increased stress and strain caused by the varus moment due to alignment could contribute to the initiation and progression of OA and has not been previously studied.

Direct measurement of stress and strain at the knee cartilage in vivo is challenging, therefore the finite element method has been used to determine the stresses and strains within the knee. Previously developed finite element knee models provide significant insight into the stress and strain distribution and contact kinematics at the knee joint (Li et al., 2001; Haut Donahue et al., 2002; Andriacchi et al., 2004; Besier et al., 2005; Fernandez & Pandy 2006; Peña et al., 2006) and have been used to investigate the effect of ligament injury (Li et al., 2002; Yao et al., 2006) and meniscectomy (Zielinska & Haut Donahue, 2006; Peña et al., 2006). Many finite element studies apply simple loading conditions and do not consider subject specific physiological loading during functional activities which would provide a more realistic

representation of the actual stresses and strains within the knee joint.

In the current study, a framework similar to previously published studies (Andriacchi et al., 2004; Besier et al., 2005; Fernandez & Pandy, 2006) was used which incorporates live human kinematics and kinetic data with subject specific finite element knee models to observe the contact variables at the knee cartilage. The loading conditions in the finite element models were determined using an inverse dynamic analysis and a muscle force reduction model with subject specific motion analysis and force platform data. The link between the tibiofemoral angle and OA progression has been well established. However, quantifying the differences in stress and strain based on the frontal plane tibiofemoral alignment with a finite element study has not been performed in any previous research. The current model demonstrated the importance of applying the varus/valgus moment at the knee, which previous finite element investigations have neglected, to determine a more realistic stress and strain distribution at the knee joint. The main goal of this study was to use subject specific loading conditions and knee joint geometry to determine the role of the frontal plane tibiofemoral angle on the magnitude of the normal stress, Tresca shear stress and normal strain of the knee cartilage.

Methods

Three healthy individuals with no history of knee OA or prior knee injury were recruited from the Northeastern University community for this study. The subjects included one male and two females (21–25 years old). Subjects of different body weight were used but the results from the finite element models were normalized by body weight to isolate the effect of the frontal plane

tibiofemoral angle. Institutional Review Board approval was obtained for experiments along with signed consent from the subjects.

Motion Analysis and Force Platform Experiments

Kinematic and kinetic data were collected with a six camera motion analysis system (EvaRT 5.0, Motion Analysis Corporation, Santa Rosa, CA) with a capture rate of 120 Hz. Two force platforms (models OR6-6-2000, OR6-7-2000, Advanced Mechanical Technology, Inc., Waltham, MA) were used and time synchronized with the motion cameras with data sampled at 1,200 Hz. The markers were placed on bony landmarks of the body and large regions of muscles were avoided to minimize the error which may occur as the markers move with the skin. The markers were placed on the leg the subjects would use to kick a ball at the (1) anterior superior iliac spine (ASIS), (2) the greater trochanter (3, 4) the lateral and medial femoral condyles, (5, 6) lateral and medial malleoli, (7) the head of the second metatarsal and (8) on the back at the second sacral vertebra of the spine (S2). Experiments for individual subjects were performed on the same day to reduce the error between trials that could occur in call-back or follow-up sessions when marker placement could affect the results (Vander Linden et al., 1999).

The subject performed three trials of static double-leg and single-leg stance for 10 s intervals. During the double leg-stance condition, the subjects were told to stand with their weight evenly distributed with the second metatarsal of the two feet approximately 30 cm apart. The experiments were monitored in real time to ensure even weight distribution over each leg. The mechanical axis of the femur in the frontal plane was defined with the marker at the ASIS and the virtual marker at the knee joint center (defined as the midpoint between the lateral and medial femoral condyles) and the mechanical axis of the tibia was defined with the virtual marker at the ankle joint center (defined as the midpoint of the lateral and medial malleoli) to the virtual marker at the knee joint center, similar to previous studies which used markers and motion analysis to define the frontal plane angle (Ford et al. 2003; Hewett et al., 2005; Myer et al. 2006; Sell et al. 2006). The tibiofemoral angle θ was assessed while the subjects were in this standard double-leg stance to ensure minimal rotation of the tibia (Hsu et al. 1988; Chao et al., 1994). During gait, the frontal plane angle may vary during different phases of single-leg support, therefore, the double-leg stance was used to assess the frontal plane tibiofemoral angle and to define a standard procedure that may be used in future studies that may use subjects (such as the elderly and advance OA individuals) who may find it difficult to balance on one leg. Fluoroscopy is an additional method which has been used to identify the tibiofemoral alignment and may provide more accuracy but it is expensive and exposes the subjects to radiation. However, the measurements in this system were accurate within 2 mm. For the single-leg stance condition, the subjects were told to

balance their weight on the leg covered with the reflective markers. The subjects were allowed to practice to become familiar to the procedure and to align themselves with the global coordinate system.

Knee Joint Reactions

An inverse dynamic analysis was used to calculate the knee joint reactions forces and moments. Furthermore, the contribution of the muscle forces was determined using a muscle force reduction method similar to previous studies by Morrison (1968, 1969, 1970) and Schipplein & Andriacchi (1991). In summary, the muscles across the knee are reduced into three groups (hamstrings, quadriceps and gastrocnemius groups) and the line of action and location of the muscles with respect to the center of the knee joint were taken from the literature (Kellis & Baltzopoulos, 1999) and balanced the external flexion/extension moment obtained from the inverse dynamic analysis to obtain the muscle force contributions. The overall muscle force contributions represent a minimum due to the absence of co-contraction in the reduction model. The muscle forces did not oppose the internal/external moment and varus/valgus knee moment. The varus knee moment present in single-leg stance was opposed by the lateral collateral ligament in the finite element models. In this investigation, only single-leg static stance was used to determine the knee joint reactions to define the loading conditions in the finite element simulations but this method has been successfully used to define the loading conditions during the stance phase of the gait cycle (Canavan et al., 2008).

Three-Dimensional Finite Element Models

Subject specific three-dimensional finite element knee models were created from sagittal view MRI. The MRI were obtained from Weymouth MRI in Weymouth, MA using a short bore, high-field 1.5-tesla MRI and a fat suppressed fast spin echo sequence with a with TE = 10 ms; TR = 536 ms, 160 mm \times 160 mm field of view and slice thickness of 2 mm with 256 \times 256 matrix and approximately 50 images. Subjects were unloaded for 30 min and brought into the MRI room in a wheel chair. The MRI were taken of the subject in the supine, nonload bearing position and a scan time of approximately 40 min. MRI were taken in the early morning to avoid the day long weight bearing of the knee joint.

The method used to construct the three-dimensional models is similar to previous published investigations utilizing three-dimensional knee models for contact kinematics analysis (Li et al., 2005; DeFrate et al., 2004) and FEA studies (Li et al., 1999, 2001, 2002). The boundaries of the bones (femur, tibia and fibula), articular cartilage (femoral and tibial) and meniscus were digitized in each 2-D MRI using the solid modeling program Rhinoceros (Rhinoceros 3.0, Seattle, Washington) to create three-dimensional point clouds. The three-dimensional point cloud was used to define the three-dimensional surface

geometry of the individual knee components which included the bones, articular cartilage, meniscus and ligaments, Figure 1A.

Li et al. (2001) showed that variation could occur in the cartilage thickness due to different investigators manually digitizing the cartilage boundaries, leading to different contact stresses in finite element simulations. It was observed that changes in the cartilage thickness of 5% led to changes in the surface cartilage pressure of 4.5%. To minimize variation and error in the models, every effort was made to follow the correct procedure to ensure accurate and precise digitization. The boundary points were placed at increments no larger than 1 mm. This method is a tedious and time consuming task and is one reason only three models were used for comparison in this investigation. In the current procedure, the thickness of the cartilage in the three-dimensional models was compared with the MRI and a maximum difference of the thickness was no greater than 3.76% and an average difference less than 1.50%.

In this investigation, static single-leg stance finite element simulations were performed with the tibia and the fibula fixed in all translations and rotations. Double-leg stance was used to define a standard method to measure the frontal plane tibiofemoral angle but it was not modeled because there is essentially no varus/valgus knee moment due to the double-leg support. Initial position of the bone at full extension was based on the MRI. The femur was held fixed at 0° flexion and all other translations and rotations were unconstrained. The forces F_z , F_y and moment M_y were applied to the femur at the midpoint of the transepicondylar axis in finite element simulations, Figure 2A. This point was chosen because studies have shown that there is a fixed axis in the femur that defines extension/flexion during gait and this axis is very closely approximated by the transepicondylar axis (Churchill et al., 1998). The transepicondylar axis is defined anatomically as the line passing through the apexes of the medial and lateral femoral epicondyles (Churchill et al., 1998). The loading conditions for the finite element models were defined with the inverse dynamic analysis and the muscle force reduction model, Table 1. The varus moment increased with increased varus alignment due to the larger moment arm from the knee joint center to the ground reaction force vector.

The three-dimensional knee models were exported into the finite element software package, ABAQUS standard v 6.5–6 (Simulia, Providence, RI, USA). Although an explicit analysis in ABAQUS may provide an easier method to reach model convergence, an implicit analysis provides more accurate results in terms of the stress and strain in the model.

The bones were modeled as rigid elements, since they are much stiffer (Cowin, 1989; Martin et al., 1998) compared with the cartilage and meniscus, and meshed with 4-node bilinear rigid quad elements. Modeling the bones as rigid has been shown to have negligible effect on the contact results (< 2%) and drastically saves computational time (Haut Donahue et al., 2002).

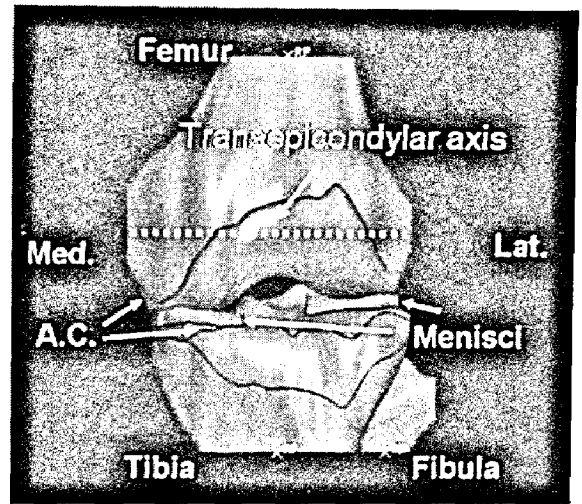


Figure 2 — Three-dimensional geometry of the left knee, which includes femur, tibia, fibula, articular cartilage and lateral and medial menisci and was used in finite element simulations.

Table 1 Subject tibiofemoral angle, weight and loading conditions for the finite element model. The axial compressive load, F_z , and posteriorly directed shear load, F_y , are a summation of the reaction forces and internal muscle force and M_y represents the varus knee moment.

Subject	Tibiofemoral Angle	Weight (N)	F_z (N)	F_y (N)	M_y (N·m)
1 Varus	0.20°	640	-822	-212	-24.68
2 Normal	7.67°	725	-930	-244	-23.26
3 Valgus	10.34°	704	-854	-164	-22.18

For the cartilage and the meniscus, a free meshing technique was used with 4-node linear tetrahedron elements. Modeling of the articular cartilage has varied from study to study. Many studies assume cartilage to behave as a linear elastic material (Li et al., 1999, 2001, 2002; Haut Donahue et al., 2002; Zielinska & Haut Donahue, 2006; Peña et al., 2006). These assumptions are justified considering the elastic response of cartilage during activities involving loading frequencies greater than 1 Hz, such as walking or stair climbing (Besier et al., 2005). In this investigation the cartilage was modeled as one layer isotropic, elastic and rigidly attached to the bone surface and the meniscus was modeled as transversely isotropic elastic with material properties taken from previously published studies based on experimental data, Table 2 (Shepherd & Seedhom, 1999; Haut Donahue et al., 2002; Zielinska & Haut Donahue, 2006).

The meniscus was attached to the tibial plateau at the meniscal horns using a set of linear spring elements similar to the methods used by Haut Donahue et al. (2002). At each horn attachment, ten linear springs with a stiffness

Table 2 Material properties used in the finite element simulations for the cartilage and the meniscus

Part	Material Properties
Cartilage	Isotropic elastic: $E = 15 \text{ MPa}$, $\nu = 0.45$
Meniscus	Transversely isotropic elastic: $E_1 = E_3 = 20 \text{ MPa}$, $E_2 = 120 \text{ MPa}$, $\nu_{13} = 0.2$, $\nu_{12} = \nu_{23} = 0.3$ $G_{12} = G_{23} = 57.7 \text{ MPa}$, $G_{13} = 8.33 \text{ MPa}$

of 200 N/mm attached the horn to the tibial plateau. The total stiffness for each horn attachment was 2000 N/mm. A transverse ligament was modeled as a linear spring with a stiffness of 900 N/mm and attached the anterior horns of the lateral and medial menisci.

The anterior cruciate ligament (ACL), posterior cruciate ligament (PCL), medial collateral ligament (MCL) and lateral collateral ligament (LCL) were modeled as one-dimensional nonlinear spring elements. The properties of each ligament were taken from the literature (Blankevoort et al., 1991) and contact was neglected between the ligaments and the other knee components.

The force-displacement relationship used to model the ligaments as nonlinear springs was defined using the piecewise function (Blankevoort et al., 1991):

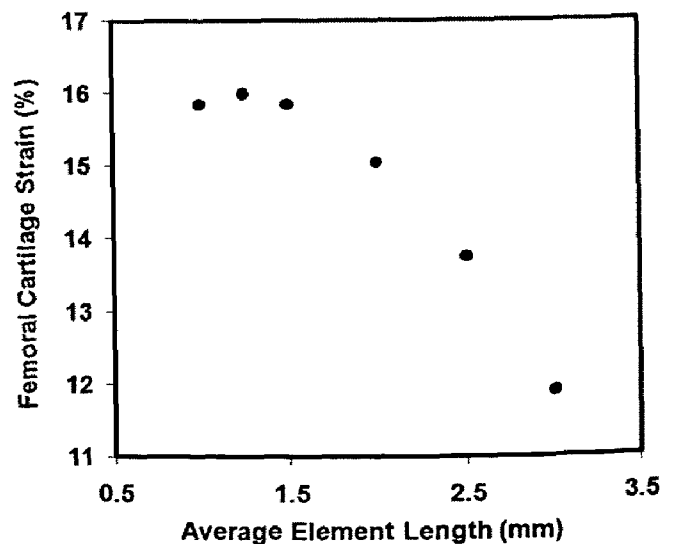
$$f = \begin{cases} \frac{1}{4} k \varepsilon^2 / \varepsilon_r & 0 \leq \varepsilon \leq 2\varepsilon_r \\ k(\varepsilon - \varepsilon_r) & \varepsilon > 2\varepsilon_r \\ 0 & \varepsilon < 0 \end{cases}$$

where f is the applied force, k is the ligament stiffness parameter, ε_r is the nonlinear strain parameter and ε is the strain in the ligaments calculated from $\varepsilon = (L - L_o) / L_o$, where L is the ligament length and L_o is the zero-load length of the ligament. The zero-load length of the element was estimated from $L_o = L_r / (\varepsilon_r + 1)$, where L_r is the ligament initial length from the MRI and ε_r is the reference strain that was found experimentally by Blankevoort et al. (1991). The stiffness parameter and reference strain ε_r were inputs into the ligament model and were taken from the literature, Table 3. Positive values of ε_r corresponded to initial tension while negative values corresponded to initially slack ligament bundles.

An average element length of 1.25 mm was used after a model convergence analysis was performed. Model convergence was tested by recording the contact variables (normal stain, normal stress, Tresca shear stress and contact force) in the cartilage for various average mesh length size. Parts were meshed with tetrahedron elements with average side length of 1.0, 1.25, 1.5, 2.0, 2.5, 3.0 mm. Adjusting the average mesh size length from 1.25 mm to 1.0 mm changed maximum strain approximately 0.10%, Figure 3. All other contact variables changed by

Table 3 Material properties of the ligaments used in the finite element model from Blankevoort et al. (1991)

Ligament	Bundle	Stiffness parameter,	
		k (N)	ε_r
Anterior Cruciate	Anterior	5000	0.06
	Posterior	5000	0.1
Posterior Cruciate	Anterior	9000	-0.24
	Posterior	9000	0.03
Lateral Collateral	Anterior	2000	-0.25
	Superior	2000	-0.05
	Posterior	2000	0.08
Medial Collateral	Anterior	2750	0.04
	Inferior	2750	0.04
	Posterior	2750	0.03

**Figure 3** — Model convergence analysis showing the maximum compressive strain in the knee cartilage with changes in the average element length. A final mesh size length of 1.25 mm was chosen for all models.

no more than 4.8%. Contact was defined between surfaces with a friction coefficient of 0.002 which was taken from a previously published study (Charnley, 1960).

The finite element results that were obtained included the distribution of the total normal knee force distributed to the medial and lateral compartments, the normal stress, Tresca shear stress and normal strain. The force distribution was of interest because the varus knee moment is key factor in the force distribution at the knee and increased tibiofemoral alignment was expected to lead to greater force distributes to the medial knee compartment. The normal stress and strain are of interest because experimental studies have related cartilage damage with the magnitude of the normal stress and strain (Repo & Finlay

1977; Kerin et al., 1998; Chen et al., 2003; Clements et al., 2001; Quinn et al., 2001). Other studies have shown that the shear stress is associated with increase catabolic factors and decrease cartilage biosynthetic activity and lead to cartilage damage and subsequent OA (Andriacchi et al., 2004).

Results

From finite element results, the percentage of the total normal knee force distributed to the medial compartment of the knee was greatest for the varus aligned individual due to the greater varus knee moment during single-leg support, Figure 4. The greater force distributed to the medial compartment led to all subjects exhibiting a larger normal stress distribution on the medial cartilage compared with the lateral cartilage, Figure 5. The stresses in the cartilage are of interest in this investigation but the meniscus is shown to observe the increased stress distribution in the medial meniscus compared with the lateral meniscus. Subject 2 (normal alignment) had the largest normal stress on the cartilage of the three different subjects due to the greater body weight and, therefore, greatest axial load and posterior load applied to the finite element model, Table 4. However, normalizing the maximum normal stress by the subject specific body weight revealed increased varus alignment led to a greater value of the maximum normal stress to the medial knee compartment in the femoral cartilage and increased valgus alignment led to a larger normalized maximum normal stress on the lateral femoral cartilage, Figure 6A. A similar trend was observed on the tibial cartilage; however,

Subject 2 (normal) exhibited the largest normal stress on the medial tibial cartilage and the smallest normal stress on the lateral tibial cartilage, Figure 6B.

The Tresca shear stress distribution also showed a greater area and magnitude on the medial compartment of the knee compared with the lateral compartment of the knee, Figure 7. Normalizing the maximum Tresca stress by body weight showed increased values on the medial cartilage in both the femoral cartilage, and tibial cartilage with increased varus alignment, Figure 8. The normalized maximum Tresca stress increased on the lateral knee compartment with increased valgus alignment, with exception of Subject 2 having the largest normalized Tresca stress on the lateral femoral cartilage compared with Subject 1 and 3. The meniscus showed larger Tresca stress concentration on the meniscus compared with the cartilage due to the large stiffness in the circumferential direction, Figure 7.

Table 4 Maximum values (in megapascals) of the normal stress on the cartilage for each of the subjects. The larger value of the normal stress occurred on the medial knee compartment due to the varus knee moment.

Subject	Medial Cartilage		Lateral Cartilage	
	Femur	Tibia	Femur	Tibia
1	5.35	5.56	2.72	2.9
2	5.91	6.34	3.17	2.68
3	5.13	5.33	3.13	3.84

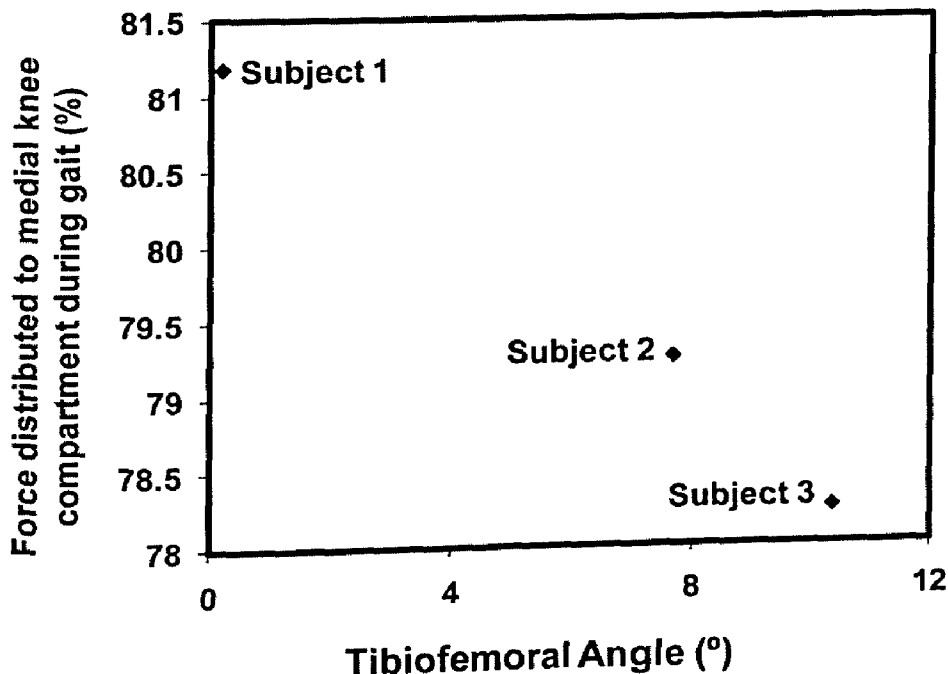


Figure 4 — The percentage of the total normal knee force distributed to the medial knee compartment during single-leg stance obtained from the finite element models for the different subjects. Subject 1 is varus alignment, Subject 2 is normal alignment and Subject 3 is valgus alignment.

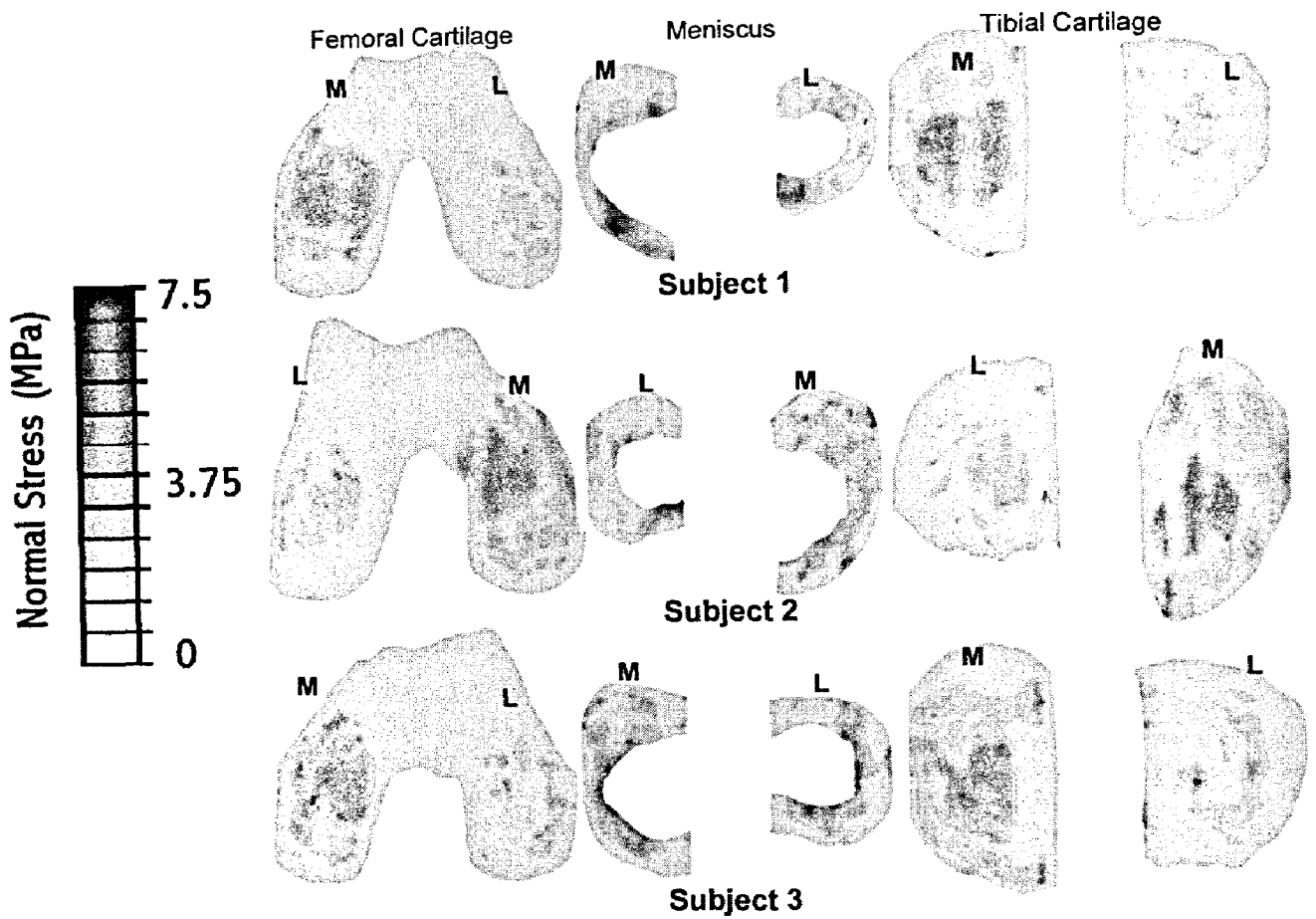


Figure 5 — Normal stress distribution in the femoral cartilage, meniscus and tibial cartilage for the left knee of Subject 1, right knee of Subject 2 and the left knee of Subject 3. The medial (M) and lateral (L) compartments are identified.

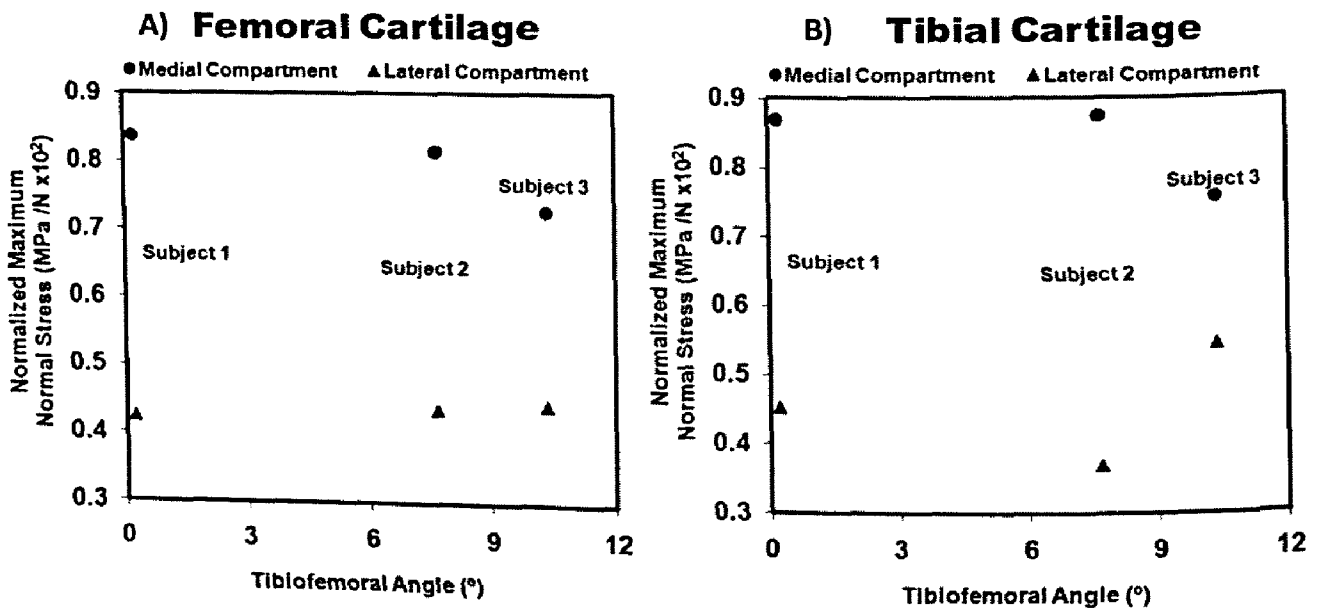


Figure 6 — The normalized maximum normal stress for each of the subjects on the medial and lateral compartment for (A) the femoral cartilage and the (B) tibial cartilage. Subject 1 is varus alignment, Subject 2 is normal alignment and Subject 3 is valgus alignment.

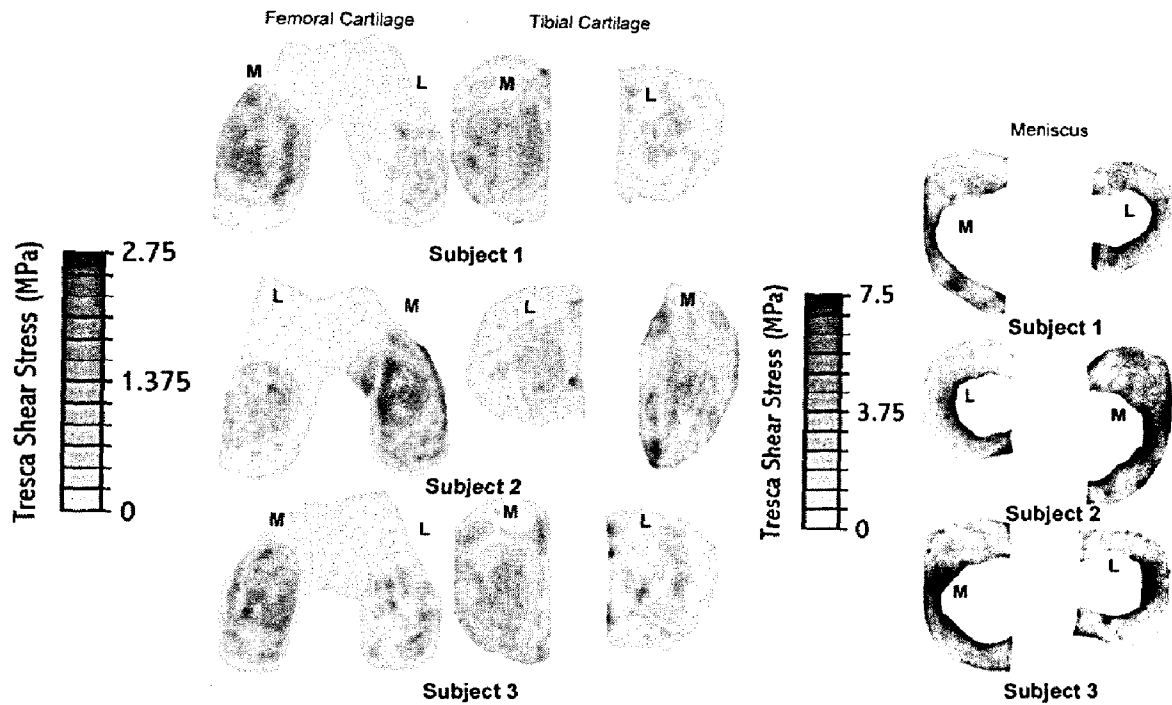


Figure 7 — The Tresca shear stress distribution in the femoral cartilage, tibial cartilage and meniscus for the left knee of Subject 1, right knee of Subject 2 and the left knee of Subject 3. The medial (M) and lateral (L) compartments are identified.

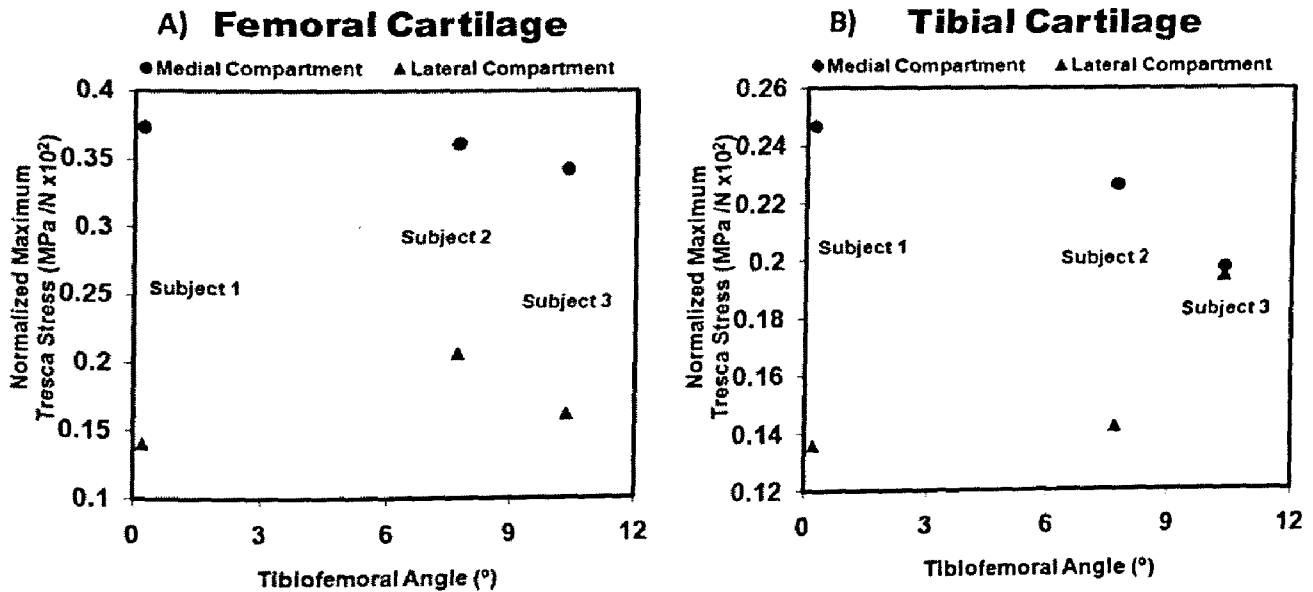


Figure 8 — The normalized maximum Tresca shear stress for each of the subjects on (A) the femoral cartilage and the (B) tibial cartilage. Subject 1 is varus alignment, Subject 2 is normal alignment and Subject 3 is valgus alignment.

Similar results were observed in the normal strain distribution in the cartilage compared with the normal stress and Tresca stress with the larger strain distribution at the medial knee compartment due to the varus knee moment at single-leg stance, Figure 9. In general, normalized maximum strain on the medial cartilage was correlated with the varus alignment, Figure 10.

Discussion

The results from this subject specific finite element investigation showed the role of the tibiofemoral angle on the stress and strain distribution at the knee joint. For each subject, the magnitude of the normal stress, Tresca stress and normal strain was largest on the medial knee

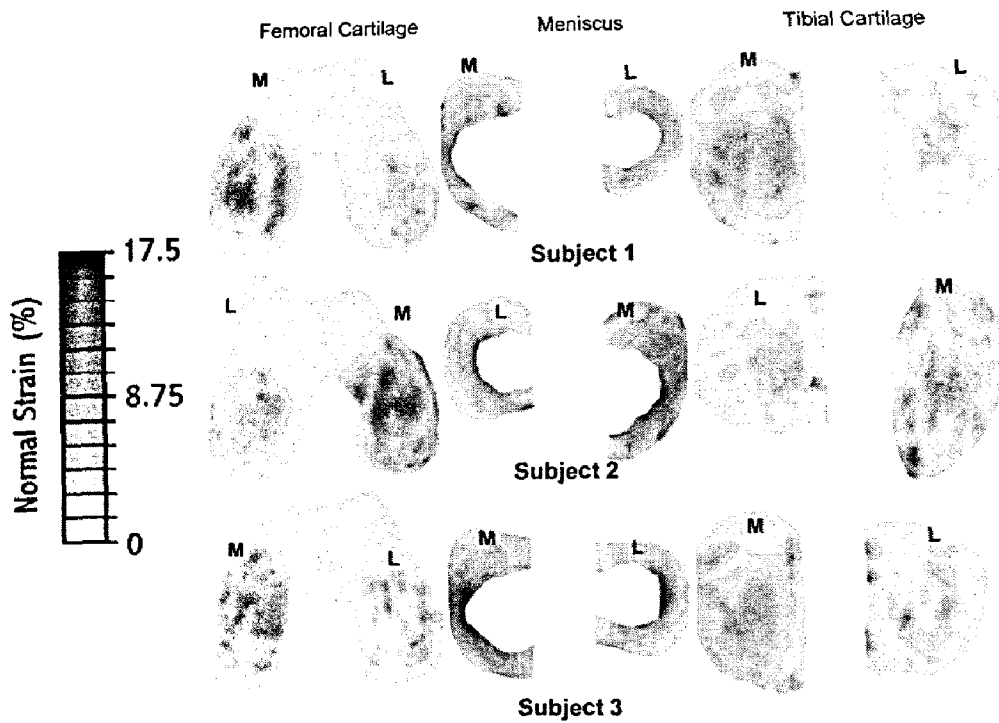


Figure 9 — Normal strain distribution in the femoral cartilage, meniscus and tibial cartilage for the left knee of Subject 1, right knee of Subject 2 and the left knee of Subject 3. The medial (M) and lateral (L) compartments are identified.

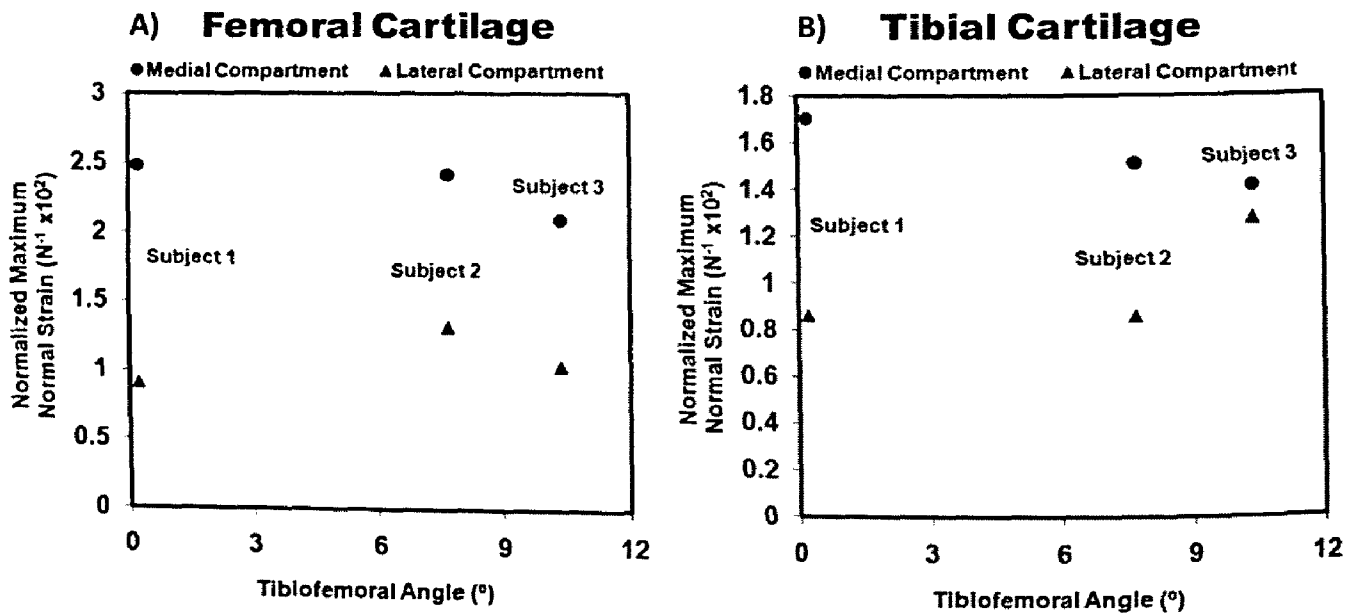


Figure 10 — The normalized maximum normal strain for each of the subjects versus the frontal plane tibiofemoral angle for (A) the femoral cartilage and the (B) tibial cartilage. Subject 1 is varus alignment, Subject 2 is normal alignment and Subject 3 is valgus alignment.

compartment due to the presence of the varus moment regardless of alignment at the knee during single-leg support. As mentioned previously, during single-leg support, approximately 70–75% of the load passes to the medial compartment of the knee joint due to the varus moment. Each subject exhibited greater than 75% of the load to the medial compartment of the knee, Figure 5, which could

be attributed to the LCL acting as the only structure to oppose the external varus moment. Including the muscle forces in the frontal plane may decrease the distribution of the total knee force to the medial knee compartment. Neglecting the contribution of the frontal plane muscles forces is a limitation of this study; however, an optimization method would be needed to calculate the frontal

plane muscle force contributions due to the number of muscles, line of action of the muscles and muscle moment arms that lead to a large number of variables. These results are different from those of Haut Donahue et al. (2002), who calculated an even force distribution between the medial and lateral knee compartments when applying an axial compressive load of 800 N to a three-dimensional finite element knee model. This research shows the importance of applying the varus knee moment in finite element knee models for properly evaluating normal forces to the medial and lateral compartment of the knee joint.

The application of the varus knee moments also led to each subject demonstrating a larger magnitude of stress and strain on the medial cartilage compared with the lateral cartilage. Peña et al. (2006) applied only an axial compressive load of 1150 N and an anterior tibial load of 134 N to a three-dimensional knee model and found maximum normal stress of 3.11 MPa on the lateral femoral cartilage and 2.68 MPa on the medial cartilage. The magnitude of the normal stresses on the medial knee cartilage was double with the application of the varus knee moment in the current model. This illustrates the importance of including the varus knee moment, when studying knee biomechanics and may explain why knee OA occurs more frequently on the medial compartment of the knee compared with the lateral compartment (Sharma et al. 2000).

Another goal of this investigation was to observe the role in the frontal plane tibiofemoral alignment, and thus the magnitude of the varus moment, during static single-leg stance on the normal stress, Tresca shear stress and normal strain at the knee cartilage based on subject specific data. Normalizing the results by subject body weight demonstrated that increased varus alignment led to increase in the stress and strain on the medial knee cartilage. On the lateral cartilage, the valgus aligned individual had the largest value of the stress and strain compared with the normal aligned individual and the varus aligned individual. The results also showed increased valgus alignment led to smaller differences in the maximum values of the stress and strain between the medial and lateral cartilage. The more uniform stress distribution and the smaller values of the overall maximum stress on either side of the knee could explain why Harman et al. (1998) showed that the wear patterns on the tibial plateau for varus and valgus malaligned individuals showed valgus knees appeared to wear out in a more uniform fashion, and this corresponds with clinical observation that patients can tolerate knee OA in a valgus alignment with better knee function for longer periods of time than in a varus knee alignment.

Although we focus on the contact stresses rather than the internal stresses, both may be important to the degradation of cartilage (Haut Donahue et al., 2002). No finite element study has reported the strain in the cartilage but experimental studies have shown cartilage damage can be correlated to the magnitude of strain (Repo & Finlay, 1977; Kerin et al., 1998; Quinn et al.,

2001; Clements et al., 2001; Chen et al., 2003; Morel et al., 2006) and may be an important contact variable to investigate. However, investigating the stress and strain at the cartilage bone interface may also be of interest. An additional mechanism of OA initiation may be a steep increase in the stiffness gradient at the underlying subchondral bone (Radin & Rose, 1986). Furthermore, Besier et al. (2005) showed large hydrostatic pressures occurring at the subchondral bone interface at the patella. In this investigation, the largest normal stress, Tresca stress and normal strain occurred at the surface but future investigation in the underlying stresses could provide valuable information in the pathogenesis of knee OA.

The limitation of having only three subjects makes it difficult to make generalizations of the tibiofemoral angle and the contact parameters. However, since previous studies have shown the relationship between knee OA and frontal plane tibiofemoral alignment (Griffin & Guilak, 2005; Felson & Zhang, 1998; Felson, 1999; Sowers, 2001; Sharma et al., 2000, 2001; Sharma, 2001; Cerejo et al., 2002; Englund & Lohmander, 2004) and studies have shown the magnitude of stress and strain can lead to cartilage damage and subsequent OA (Repo & Finlay, 1977; Kerin et al., 1998; Quinn et al., 2001; Chen et al., 2003; Clements et al., 2001; Morel et al., 2006), reporting the contact data based on the tibiofemoral angle and varus moment may give some insight into the role alignment plays in load distribution and possible OA initiation and progression. There is no known value of stress or strain that guarantees the development of knee OA. However, the data shows that Subject 1 would be most susceptible to developing medial compartment OA due to the larger stress and strain in the medial compartment. Subject 3 would be most susceptible to developing lateral compartment OA due to the larger stress and strain in the lateral compartment of the knee.

This is the first attempt to use subject specific kinematic and kinetic data in subject specific FEA models to quantify the difference in stress and strain with varus and valgus knee alignment. It is not known at what value of stress or strain that irreversible damage to cartilage will occur, however, the results could be used to identify individuals most susceptible to OA and prescribe preventive measures. Although only three subjects were used, investigation with more subjects could provide a better understanding of the relationship of the contact variables to the tibiofemoral alignment. Furthermore, since alignment differences may exist between genders, a gender specific study may be of interest to determine if tibiofemoral alignment affects the sexes differently.

Simple material models were used to define the properties of the cartilage and the meniscus. Poroelastic material models may be better to determine a more realistic stress distribution in the cartilage. The ligament properties were based on data available in literature. Measuring the material properties of ligaments in live subjects is both impractical and impossible. Modeling the ligaments as nonlinear springs was sufficient in this case but more complex modeling of the ligaments could be

considered. Furthermore, the finite element models were constructed based on the MRI and were not adjusted to the alignment of the individuals in stance positions. The alignment of the individuals was measured during double-leg stance and alignment may change during the supine position. Fluoroscopy techniques could be used in future investigation to align finite element models to account for the frontal plane alignment of the tibiofemoral joint.

The loading conditions represent a minimum of the total forces that the knee is exposed to during static stance. The cocontraction of the muscles at the knee adds a great deal of force to the knee during dynamic activities. Furthermore, the muscle forces did not add any additional support to oppose the external varus moment. The LCL was the only structure which opposed the external varus moment and including the muscles may decrease the value of the stresses and strain as well as the percentage to the total knee force distributed to the medial knee compartment.

In this investigation, subject specific models were developed and finite element analysis was performed to observe the effect of the frontal plane tibiofemoral angle on the normal stress, Tresca shear stress and normal strain at the surface of the knee cartilage. The results showed that the greatest magnitude of the normal stress, Tresca shear stress and normal strain at the medial compartment was for the varus aligned individual. Considering the lateral knee compartment, the individual with valgus alignment had the largest stress and strain at the cartilage. The results could be used clinically to identify individuals most susceptible to OA and to develop OA preventive and rehabilitation measures.

References

- Andriacchi, T.P. (1994). Dynamics of knee malalignment. *The Orthopedic Clinics of North America*, 25, 395–403.
- Andriacchi, T.P., Mündermann, A., Smith, R.L., Alexander, E.J., Dyrby, C.O., & Koo, S. (2004). A framework for the *in vivo* pathomechanics of osteoarthritis at the knee. *Annals of Biomedical Engineering*, 32, 447–457.
- Arokoski, J.P.A., Jurvelin, J.S., Vaatainen, U., & Helminen, H.J. (2000). Normal and pathological adaptations of articular cartilage to joint loading. *Scandinavian Journal of Medicine & Science in Sports*, 10, 186–198.
- Besier, T.F., Gold, G.E., Beaupre, G.S., & Delp, S.L. (2005). A modeling framework to estimate patellofemoral joint cartilage stress *in vivo*. *Medicine and Science in Sports and Exercise*, 37, 1924–1930.
- Blankevoort, L., Kuiper, J.H., Huijskes, R., & Grootenboer, H.J. (1991). Articular contact in a three-dimensional model of the knee. *Journal of Biomechanics*, 24, 1019–1031.
- Canavan, P., Yang, N.H., & Nayeb-Hashemi, H. (2008). Method to Determine the Effect of the frontal plane tibiofemoral angle on the varus-valgus moment at the knee during stance and gait. *Proceedings of ASME Summer Bioengineering Conference*, 2008(June), 25–29 Marco Island, Florida, USA.
- Cerejo, R., Dunlop, D.D., Cahue, S., Channin, D., Song, J., & Sharma, L. (2002). The influence of alignment on risk of knee osteoarthritis progression according to baseline stage of disease. *Arthritis and Rheumatism*, 46, 2632–2636.
- Chao, E.Y.S., Neluheni, E.V.D., Hsu, R.W.W., & Paley, D. (1994). Biomechanics of malalignment. *The Orthopedic Clinics of North America*, 25, 379–386.
- Charnley, J. (1960). The lubrication of animal joints in relation to surgical reconstruction by arthroplasty. *Annals of the Rheumatic Diseases*, 19, 10–19.
- Chen, C.-T., Bharagava, M., Lin, P.M., & Torzilli, P.A. (2003). Time, stress and location dependent chondrocyte death and collagen damage in cyclically loaded articular cartilage. *Journal of Orthopaedic Research*, 21, 888–898.
- Churchill, D.L., Incavo, S.J., Johnson, C.C. & Beynon, B.D. (1998). The transepicondylar axis approximates the optimal flexion axis of the knee. *Clinical Orthopaedics & Related Research*, 356, 111–118.
- Clements, K.M., Bee, Z.C., Crossingham, G.V., Adams, M.A., & Sharif, M. (2001). How severe must repetitive loading be to kill chondrocytes in articular cartilage? *Osteoarthritis and Cartilage*, 9, 499–507.
- Cooper, C., Snow, S., McAlindon, T.E., Kellingray, S., Stuart, B., Coggon, D., et al. (2000). Risk factors of the incidence and progression of radiographic knee osteoarthritis. *Arthritis and Rheumatism*, 43, 995–1000.
- Cowin, S.C. (1989). *Bone Mechanics*. Boca Raton: CRC Press.
- DeFrate, L.E., Sun, H., Gill, T.J., Rubash, H.E., & Li, G. (2004). *In vivo* tibiofemoral contact analysis using 3D MRI-based knee models. *Journal of Biomechanics*, 37, 1499–1504.
- Englund, M., & Lohmander, L.S. (2004). Risk factors for symptomatic knee osteoarthritis fifteen to twenty-two years after meniscectomy. *Arthritis and Rheumatism*, 50, 2811–2819.
- Felson, D.T., & Zhang, Y. (1998). An update on the epidemiology of knee and hip osteoarthritis with a view to prevention. *Arthritis and Rheumatism*, 41, 1343–1355.
- Felson, D.T., Conference Chair. (1999). Osteoarthritis: new insights. part 1: the disease and its risk factors. *Annals of Internal Medicine*, 133, 635–646.
- Felson, D.T. (2005). The sources of pain in knee osteoarthritis. *Current Opinion in Rheumatology*, 17, 624–628.
- Fernandez, J.W., & Pandy, M.G. (2006). Integrating modeling and experiments to assess dynamic musculoskeletal functions in humans. *Experimental Physiology*, 91, 371–382.
- Ford, K.R., Myer, G.D., & Hewett, T.E. (2003). Valgus knee motion during landing in high school female and male basketball players. *Medicine and Science in Sports and Exercise*, 35, 1745–1750.
- Griffin, T.M., & Guilak, F. (2005). The role of mechanical loading in the onset and progression of osteoarthritis. *Exercise and Sport Sciences Reviews*, 33, 195–200.
- Harman, M.K., Markovich, G.D., Banks, S.A., & Hodge, W.A. (1998). Wear patterns on tibial plateaus from varus and valgus osteoarthritic knees. *Clinical Orthopaedics and Related Research*, 352, 149–158.
- Haut Donahue, T.L., Hull, M.L., Rashid, M.M., & Jacobs, C.R. (2002). A finite element model of the human knee joint for the study of tibio-femoral contact. *Journal of Biomechanical Engineering*, 124, 273–280.
- Hewett, T.E., Myer, G.D., Ford, K.R., Heidt, R.S., Colosimo, A.J., McLean, S.G., et al. (2005). Biomechanical measures of neuromuscular control and valgus loading of the knee predict anterior cruciate ligament injury risk in female athletes. *American Journal of Sports Medicine*, 33, 492–501.
- Hsu, R.W., Himeno, S., Coventry, M.B., & Chao, E.Y.S. (1988). Normal axial alignment of the lower extremity and load-bearing distribution at the knee. *Clinical Orthopaedics and Related Research*, 255, 215–227.

- Johnson, F., Leitzl, S., & Waugh, W. (1980). The distribution of load across the knee. A comparison of static and dynamic measurements. *The Journal of Bone and Joint Surgery. British Volume*, 62-B, 346–349.
- Karachalios, T., Sarangi, P.P., & Newman, J.H. (1994). Severe varus and valgus deformities treated by total knee arthroplasty. *The Journal of Bone and Joint Surgery. British Volume*, 76-B, 938–942.
- Kellis, E., & Baltzopoulos, V. (1999). *In vivo* determination of the patella tendon and hamstrings moment arms in adult males using videofluoroscopy during submaximal knee extension and flexion. *Clinical Biomechanics (Bristol, Avon)*, 14, 118–124.
- Kerin, A.J., Wisnom, M.R., & Adams, M.A. (1998). The compressive strength of articular cartilage. *Proceedings of the Institution of Mechanical Engineers, Part H: Journal of Engineering in Medicine*, 212, 273–280.
- Li, G., Gil, J., Kanamori, A., & Woo, S.L.-Y. (1999). A validated three-dimensional model of a human knee joint. *Journal of Biomechanical Engineering*, 121, 657–662.
- Li, G., Lopez, O., & Rubash, H. (2001). Variability of a three-dimensional finite element model constructed using magnetic resonance images of a knee for joint contact stress analysis. *Journal of Biomedical Engineering*, 123, 341–346.
- Li, G., Suggs, J., & Gill, T. (2002). The effect of anterior cruciate ligament injury on knee joint function under a simulated muscle load: a three-dimensional computational simulation. *Annals of Biomedical Engineering*, 30, 713–720.
- Li, G., DeFrate, L.E., Park, S.E., & Gill, T.J. (2005). *In vivo* articular cartilage contact kinematics of the knee: an investigation using dual-orthogonal fluoroscopy and magnetic resonance image-based computer models. *American Journal of Sports Medicine*, 33, 102–107.
- Martin, R.B., Burr, D.B., & Sharkey, N.A. (1998). *Skeletal tissue mechanics*. New York: Springer-Verlag.
- Morel, V., Berutto, C., & Quinn, T.M. (2006). Effects of damage in the articular surface on the cartilage response to injurious compression *in vitro*. *Journal of Biomechanics*, 39, 924–930.
- Morrison, J.B. (1968). Bioengineering analysis of force actions transmitted by the knee joint. *Biomedical Engineering*, 3, 164–170.
- Morrison, J.B. (1969). Function of the knee joint in various activities. *Biomedical Engineering*, 4, 473–480.
- Morrison, J.B. (1970). The mechanics of the knee joint in relation to normal walking. *Journal of Biomechanics*, 3, 51–61.
- Myer, G.D., Ford, K.R., McLean, S.G., & Hewett, T.E. (2006). The effects of polymetric versus dynamic stabilization and balance training on lower extremity biomechanics. *American Journal of Sports Medicine*, 34, 445–455.
- Peña, E., Calvo, B., Martínez, M.A., & Doblaré, M. (2006). A three-dimensional finite element analysis of the combined behavior of ligaments and menisci in the healthy human knee joint. *Journal of Biomechanics*, 39, 1686–1701.
- Quinn, T.M., Allen, R.G., Schalet, B.J., Perumbuli, P., & Huniker, E.B. (2001). Matrix and cell injury due to sub-impact loading of adult bovine articular cartilage explants: Effects of strain rate and peak stress. *Journal of Orthopaedic Research*, 19, 242–249.
- Radin, E.L., & Rose, R.M. (1986). Role of subchondral bone in the initiation and progression of cartilage damage. *Clinical Orthopaedics and Related Research*, 213, 34–40.
- Repo, R.U., & Finlay, J.B. (1977). Survival of articular cartilage after controlled impact. *The Journal of Bone and Joint Surgery. American Volume*, 59, 1068–1076.
- Schipplein, O.D., & Andriacchi, T.P. (1991). Interaction between active and passive knee stabilizers during level walking. *Journal of Orthopaedic Research*, 9, 113–119.
- Sell, T.C., Ferris, C.M., Abt, J.P., Tsai, Y-S., Myers, J.B., Fu, F.H., et al. (2006). The effect of direction and reaction on the neuromuscular and biomechanical characteristics of the knee during tasks that simulate the noncontact anterior cruciate ligament injury mechanism. *American Journal of Sports Medicine*, 34, 43–54.
- Sharma, L., Lou, C., Cahue, S., & Dunlop, D.D. (2000). The mechanism of the effect of obesity in knee osteoarthritis. *Arthritis and Rheumatism*, 43, 568–575.
- Sharma, L. (2001). Local factors in osteoarthritis. *Current Opinion in Rheumatology*, 13, 441–446.
- Sharma, L., Song, J., Felson, D.T., Cahue, S., Shamiyeh, E., & Dunlop, D.D. (2001). The role of knee alignment in disease progression and functional decline in knee osteoarthritis. *Journal of the American Medical Association*, 286, 188–195.
- Shelburne, K.B., Torry, M.R., & Pandy, M.G. (2005). Muscle, ligament, and joint-contact forces at the knee during walking. *Medicine and Science in Sports and Exercise*, 37, 1948–1956.
- Shepherd, T.E.W., & Seedhom, B.B. (1999). The 'instantaneous' compressive modulus of human articular cartilage in joints of the lower limb. *Rheumatology*, 38, 124–132.
- Sowers, M. (2001). Epidemiology of risk factors for osteoarthritis: systemic factors. *Current Opinion in Rheumatology*, 13, 447–451.
- Tetsworth, K., & Paley, D. (1994). Malalignment and degenerative arthropathy. *The Orthopedic Clinics of North America*, 25, 367–377.
- Vander Linden, D.W., Carlson, S.J., & Hubbard, R.L. (1999). Reproducibility and accuracy of angle measurements obtained under static conditions with motion analysis video system. *Physical Therapy*, 72, 300–305.
- Yao, J., Snibbe, J., Maloney, M., & Lerner, A.L. (2006). Stresses and strains in the medial meniscus of an ACL deficient knee under anterior loading: A finite element analysis with image-based experimental validation. *Journal of Biomechanical Engineering*, 128, 135–141.
- Zielinska, B., & Haut Donahue, T.L. (2006). 3D finite element model of meniscectomy: changes in joint contact behavior. *Journal of Biomechanical Engineering*, 128, 115–123.
- Zhao, D., Banks, S.A., Mitchell, K.H., D'Lima, D.D., Colwell, C.W., Jr., & Fregly, B.J. (2007). Correlation between the knee adduction torque and medial contact force for a variety of gait patterns. *Journal of Orthopaedic Research*, 25, 789–797.
- Zhao, D., Banks, S.A., Mitchell, K.H., D'Lima, D.D., Colwell, C.W., Jr., & Fregly, B.J. (2006). The relationship between the knee adduction torque and medial contact force during gait. *Proceedings of BIO2006, 2006 Summer Bioengineering Conference, June 21–25*.